

EEG-SCMM: Soft Contrastive Masked Modeling for Cross-Corpus EEG-Based Emotion Recognition

Qile Liu^{1,2}, Weishan Ye^{1,2}, Yulu Liu^{1,2}, Zhen Liang^{1,2,*}

¹School of Biomedical Engineering, Shenzhen University, Shenzhen, 518060, Guangdong, China

²Guangdong Provincial Key Laboratory of Biomedical Measurements and Ultrasound Imaging, Shenzhen, China
{liuqile2022, 2110246024, 2021220004}@email.szu.edu.cn, janezliang@szu.edu.cn

Abstract

Emotion recognition using electroencephalography (EEG) signals has garnered widespread attention in recent years. However, existing studies have struggled to develop a sufficiently generalized model suitable for different datasets without re-training (**cross-corpus**). This difficulty arises because distribution differences across datasets far exceed the intra-dataset variability. To solve this problem, we propose a novel **Soft Contrastive Masked Modeling (SCMM)** framework. Inspired by emotional continuity, SCMM integrates soft contrastive learning with a new hybrid masking strategy to effectively mine the "short-term continuity" characteristics inherent in human emotions. During the self-supervised learning process, soft weights are assigned to sample pairs, enabling adaptive learning of similarity relationships across samples. Furthermore, we introduce an aggregator that weightedly aggregates complementary information from multiple close samples based on pairwise similarities among samples to enhance fine-grained feature representation, which is then used for original sample reconstruction. Extensive experiments on the SEED, SEED-IV and DEAP datasets show that SCMM achieves state-of-the-art (SOTA) performance, outperforming the second-best method by an average accuracy of 4.26% under two types of cross-corpus conditions (same-class and different-class) for EEG-based emotion recognition.

Introduction

Emotions are human attitudinal experiences and behavioral responses to objective things, closely related to health conditions and behavioral patterns (Wang, Zhang, and Tang 2024). Compared to speech (Singh and Goel 2022), gestures (Noroozi et al. 2018), and facial expressions (Canal et al. 2022), electroencephalography (EEG) offers a more direct and objective measurement of human emotions by capturing brain activity across various scalp locations (Hu et al. 2019). Recently, researchers have increasingly emphasised EEG-based emotion recognition (Zhong, Wang, and Miao 2020; Zhao, Yan, and Lu 2021; Zhang, Liu, and Zhong 2022; Gao et al. 2024), aiming to advance the development of affective brain-computer interfaces (aBCIs). However, three critical challenges remain to be addressed in current approaches.

(1) **Dataset Specificity.** Most existing EEG-based emotion recognition methods are typically designed for a single dataset, necessitating model retraining when the dataset changes. This requirement significantly limits the model's generalizability and scalability, hindering its application across different datasets. To tackle this issue, the concept of **cross-corpus** has been proposed, which is designed to be generalized across multiple datasets. A cross-corpus model is trained on one dataset and can be directly applied to another without the need for retraining from scratch. This concept, which originated in natural language processing (Schuller et al. 2010; Zhang et al. 2011), has been extended to various domains in recent years (Rayatdoost and Soleymani 2018; Chien, Yang, and Lee 2020; Ryumina, Dresvyanskiy, and Karpov 2022). Although existing EEG-based emotion recognition methods, such as BiDANN (Li et al. 2018), TANN (Li et al. 2021), and PR-PL (Zhou et al. 2023), have achieved superior performance in within-subject or cross-subject tasks, their efficacy significantly degrades in cross-corpus scenarios, where differences in data distribution across datasets far exceed the variability within a single dataset (Rayatdoost and Soleymani 2018).

(2) **Data Availability.** Current approaches for cross-domain or cross-corpus EEG-based emotion recognition rely heavily on domain adaptation techniques, which depend extensively on the availability of labeled source data and unlabeled target data. For example, AD-TCN (He, Zhong, and Pan 2022) learned an asymmetric mapping that adapts the target domain feature encoder to the source domain, aiming to eliminate the complicated steps of target domain labeling and improve the model performance in cross-domain scenarios. Similarly, E²STN (Zhou et al. 2024) integrated content information from the source domain with style information from the target domain to create stylized emotional EEG representations. However, these methods require prior access to all labeled source data and unlabeled target data for model training, presenting a significant limitation due to data availability constraints (Liu et al. 2024a).

(3) **Ignorance of Emotional Continuity.** Unlike domain adaptation techniques, contrastive learning (CL) achieves superior performance without relying on labeled data, and has demonstrated significant potential in enhancing feature representation capabilities across various domains (Chen et al. 2020; Radford et al. 2021; Zhang et al. 2022). Current

*Corresponding author.

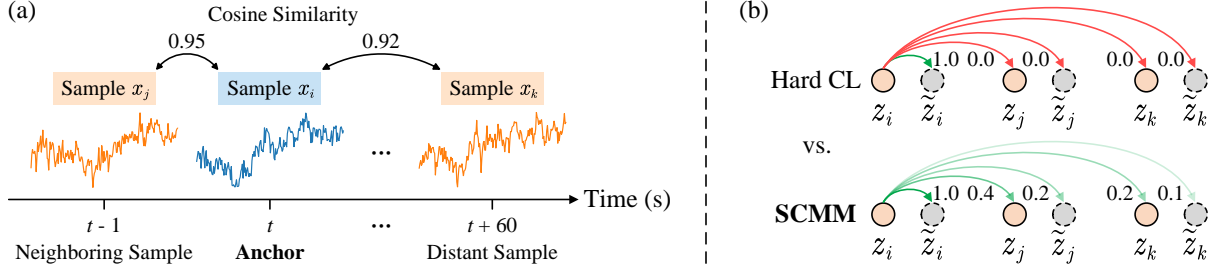


Figure 1: **(a) An illustration of emotional continuity.** We take the sample x_i at second t within an EEG trial as the anchor, and calculate the cosine similarity between x_i and its neighboring sample x_j , as well as the distant sample x_k . High cosine similarities indicate that human emotions remain relatively stable and similar over a certain period. **(b) Hard CL vs. SCMM.** Traditional hard contrastive learning considers the embeddings z_i and \tilde{z}_i of the same sample x_i and its augmented view \tilde{x}_i as positive pairs, while different samples and their augmented views are treated as negative pairs. When computing the contrastive loss, the weights for positives and negatives are set to 1 and 0, respectively. In contrast, the soft contrastive learning strategy designed in SCMM generates soft assignments for different sample pairs based on their distances in the original data space.

CL-based methods for EEG-based emotion recognition consider an anchor and its augmented views as positive pairs, while treating all other samples as negatives, as shown in Fig. 1(b) (Hard CL). For example, CLISA (Shen et al. 2022) employed contrastive learning to minimize the inter-subject differences by maximizing the similarity in EEG representations across subjects. JCFA (Liu et al. 2024a) performed joint contrastive learning across three domains to align the time- and frequency-based embeddings of the same sample in the latent time-frequency space, achieving state-of-the-art (SOTA) performance in cross-corpus scenarios. However, psychological and neuroscientific studies have shown that emotions exhibit significant “short-term continuity” characteristics (Davidson 1998; Houben, Van Den Noortgate, and Kuppens 2015). In other words, human emotions are relatively stable over certain periods, with sudden changes being rare. As illustrated in Fig. 1(a), a high cosine similarity is maintained between an anchor sample x_i and its neighboring sample x_j , and even a distant sample x_k separated by extended periods (e.g., 60 seconds). Given this nature of emotions, we propose that the definition of positive pairs in CL-based EEG analysis should extend beyond just the anchor and its augmented views. Instead, it should include a broader range of similar samples, especially those that are temporally proximal, as shown in Fig. 1(b) (SCMM). However, existing methods like JCFA (Liu et al. 2024a), which follow the traditional CL paradigm (Chen et al. 2020), may incorrectly pull apart similar but not identical samples, thus failing to capture the inherent correlations of EEG signals.

To address the aforementioned three critical issues, we propose a novel **Soft Contrastive Masked Modeling (SCMM)** framework for cross-corpus EEG-based emotion recognition. Unlike traditional hard CL shown in Fig. 1(b), SCMM considers emotional continuity and incorporates soft assignments of sample pairs. This approach enables the model to identify the fine-grained relationships between samples in a self-supervised manner, thereby enhancing the generalizability of EEG representations. Comprehensive experiments on three well-recognized datasets demonstrate

that SCMM consistently achieves SOTA performance, highlighting its superior capability and stability. In summary, the main contributions of SCMM are outlined as follows:

- Inspired by the nature of emotions, we propose a novel SCMM framework to address cross-corpus EEG-based emotion recognition. This approach assigns soft weights to sample pairs during contrastive learning to capture the similarity relationships between different samples. As a result, better feature representations of EEG signals are learned in a self-supervised manner. To the best of our knowledge, this is the first study to introduce soft contrastive learning into EEG-based emotion recognition.
- We also develop a new hybrid masking strategy to generate diverse masked samples by considering both channel and feature relationships, which is essential for enhancing contrastive learning. Additionally, we introduce an aggregator that weightedly aggregates complementary information from the embeddings of multiple close samples, enabling fine-grained feature learning and improving the model’s overall capability.
- We conduct extensive experiments on three well-known datasets (SEED, SEED-IV, and DEAP), showing that SCMM achieves consistent SOTA performance compared to eight competitive methods, surpassing the second-best method by an average accuracy of 4.26%.

Methodology

Problem Definition

Given an unlabeled pre-training EEG emotion dataset $\mathcal{X} = \{x_i\}_{i=1}^N$ with N samples, where each sample $x_i \in \mathbb{R}^{C \times F}$ contains C channels and F -dimensional features, the goal is to learn a nonlinear embedding function f_θ . This function is designed to map x_i to its representation h_i that best describes itself by leveraging the emotional continuity inherent in EEG signals. Ultimately, the pre-trained model is capable of producing generalizable EEG representations that can be effectively used across different EEG emotion datasets.

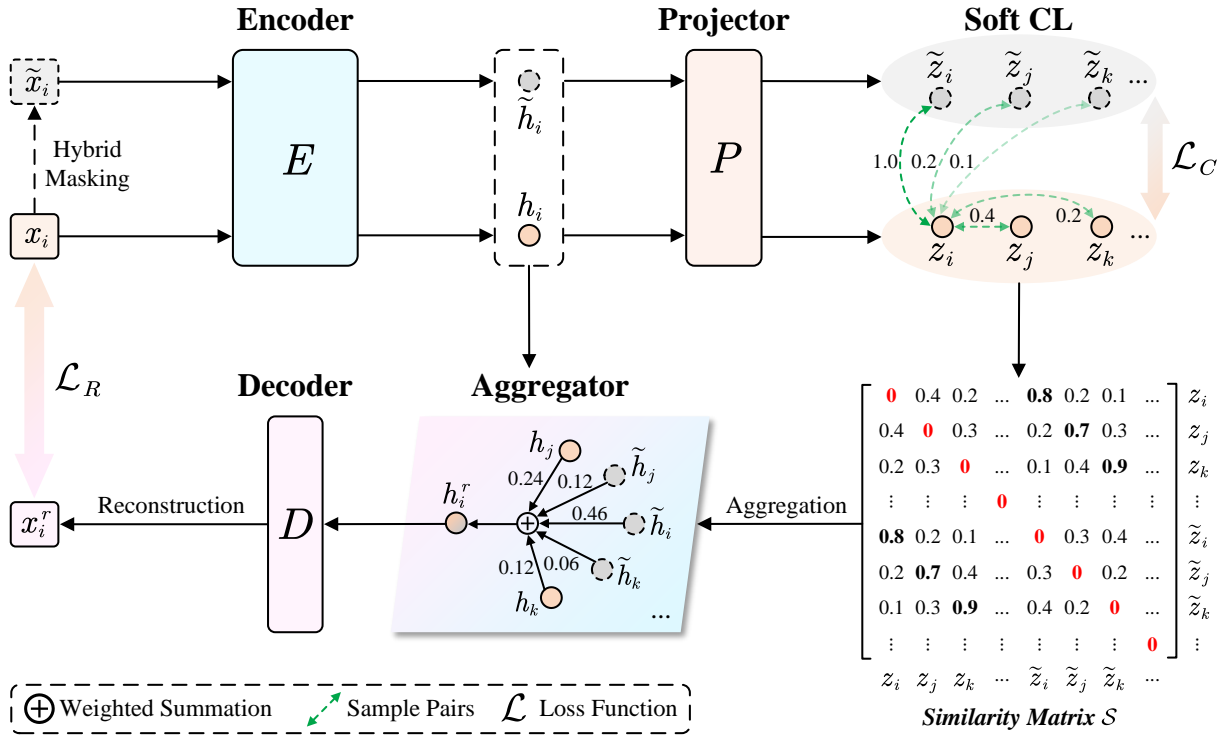


Figure 2: **The overall framework of SCMM.** The pre-training process of SCMM involves three modules: (1) hybrid masking, (2) soft contrastive learning, and (3) aggregate reconstruction.

Model Architecture

The overall framework of SCMM is illustrated in Fig. 2, which includes three main modules: hybrid masking, soft contrastive learning, and aggregate reconstruction. Below, we detail the specific design of each module and the pre-training process of SCMM.

Hybrid Masking The selection of masking strategies is crucial for CL and masked modeling (Zhang et al. 2024; Liu et al. 2024b). For an input EEG sample $x_i \in \mathcal{X}$, most existing methods use random masking (Zhang, Liu, and Zhong 2022) or channel masking (Li et al. 2022) to generate the masked sample \tilde{x}_i . The random masking strategy masks samples along the feature dimension, ignoring the inter-channel relationships of EEG signals. While a large masking ratio (e.g., 75%) can mask entire portions of certain channels, it complicates the modeling process due to significant information loss. Conversely, the channel masking strategy masks features across all dimensions of the selected channels, losing the relationships between different dimensional features. Neither approach captures both channel and feature relationships simultaneously. Therefore, we develop a new hybrid masking strategy to generate diverse masked samples by considering both channel and feature relationships.

Specifically, we first generate a random masking matrix $\text{Mask}_R \in \{0, 1\}$ with dimensions $C \times F$, and a channel masking matrix $\text{Mask}_C \in \{0, 1\}$ with dimensions $C \times F$, both derived from binomial distributions with masking ratios $r \in (0, 1)$. Here, the element values in each row of Mask_C

are either all 1s or all 0s. Next, we generate a probability matrix $U \in [0, 1]$ with dimensions $C \times 1$ for hybrid masking, which is drawn from a uniform distribution. The hybrid masking process is defined as:

$$\tilde{x}_{i,c} = \begin{cases} x_{i,c} \odot \text{Mask}_{R,c} & \text{if } \mu < U_c \leq 1 \\ x_{i,c} \odot \text{Mask}_{C,c} & \text{if } 0 \leq U_c \leq \mu \end{cases}, \quad (1)$$

where $x_{i,c}$ represents the c -th channel of x_i , and $\tilde{x}_{i,c}$ is the corresponding masked sample. \odot denotes element-wise multiplication. U_c is the probability value in the c -th row, and μ is a probability threshold that controls the weights of the two masking strategies. By integrating the hybrid masking strategy in SCMM, we enhance the diversity of masked samples, encouraging the model to learn richer and more robust feature representations that account for both channel and feature relationships within EEG signals. Figure 3 illustrates the differences between three masking strategies.

Soft Contrastive Learning Traditional hard CL treats augmented views generated from the same sample as positive pairs, and those from different samples as negative pairs (Chen et al. 2020; Eldele et al. 2021; Yue et al. 2022). During the computation of the contrastive loss, hard values (1 or 0) are assigned to sample pairs, as illustrated in Fig. 1(b) (Hard CL). However, we argue that this approach fails to account for the “short-term continuity” characteristic inherent in human emotions, leading to inaccurate modeling of inter-sample relationships and hindering the generalizability of the learned embeddings.

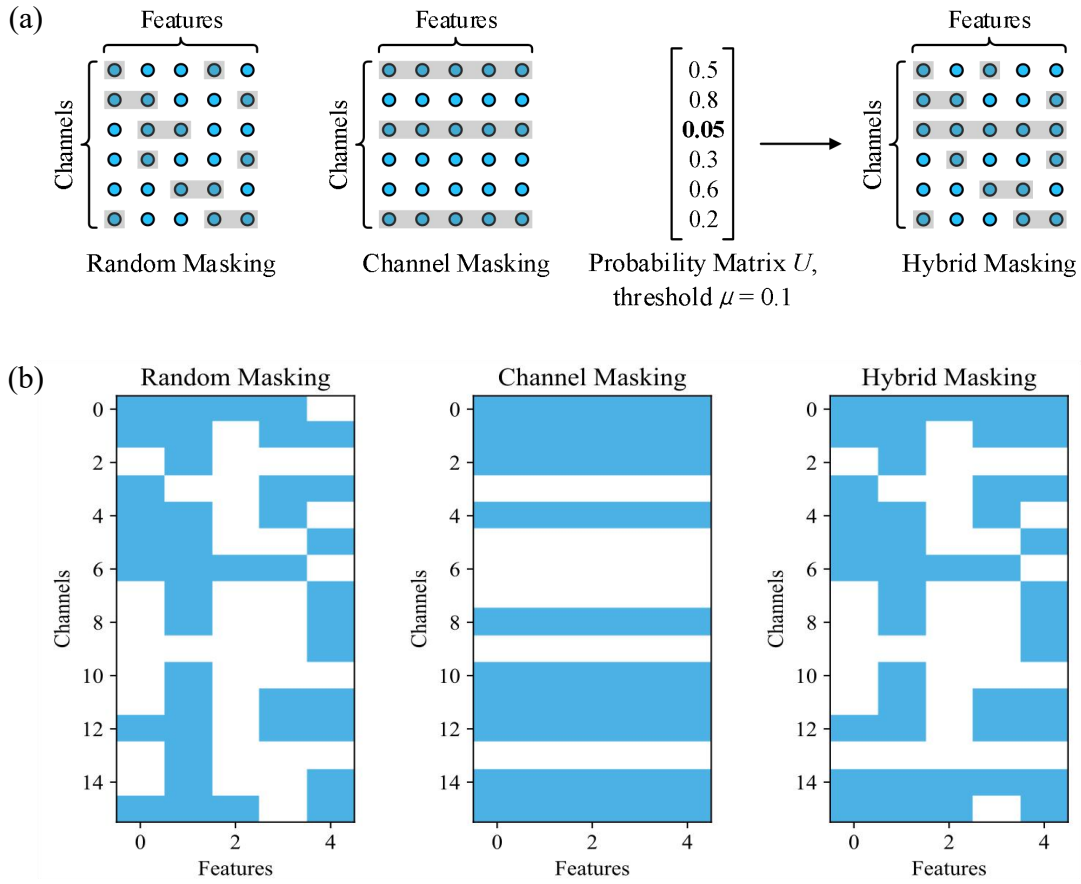


Figure 3: **Illustrations of different masking strategies.** (a) compares various masking strategies, and (b) presents examples of generated masked samples using three strategies. The masking ratio and threshold are set to $r = 0.5$ and $\mu = 0.1$, respectively.

To address this issue, we propose defining soft assignments for different sample pairs, as shown in Fig. 1(b) (SCMM). We first input x_i and \tilde{x}_i into an encoder E that maps samples to embeddings, denoted as $h_i = E(x_i)$ and $\tilde{h}_i = E(\tilde{x}_i)$. These embeddings are then projected into a latent space \mathcal{Z} using a projector P , resulting in $z_i = P(h_i)$ and $\tilde{z}_i = P(\tilde{h}_i)$. Next, we perform soft contrastive learning in \mathcal{Z} using z_i and \tilde{z}_i . Specifically, for a given pair of samples (x_i, x_j) , we first calculate the normalized distance $D(x_i, x_j)$ between x_i and x_j in the original data space as:

$$D(x_i, x_j) = \text{Norm}(\text{Dist}(x_i, x_j)) \in [0, 1], \quad (2)$$

where $\text{Dist}(\cdot, \cdot)$ is a metric function used to measure the distance between sample pairs, and $\text{Norm}(\cdot)$ denotes min-max normalization. In the experiments, we take the negative of cosine similarity as the metric function. Based on the normalized distance $D(x_i, x_j)$, we then define a soft assignment $w(x_i, x_j)$ for each pair of samples (x_i, x_j) using the sigmoid function $\sigma(x) = 1/(1 + \exp(-x))$:

$$w(x_i, x_j) = 2\alpha \cdot \sigma(-D(x_i, x_j)/\tau_w), \quad (3)$$

where $\alpha \in [0, 1]$ is a boundary parameter that controls the upper bound of soft assignments. τ_w is a sharpness parameter, where smaller values of τ_w result in greater differences

in $w(\cdot, \cdot)$ between sample pairs, and vice versa. Figure 4 depicts heat maps of soft assignments $w(\cdot, \cdot)$ under different sharpness parameters τ_w .

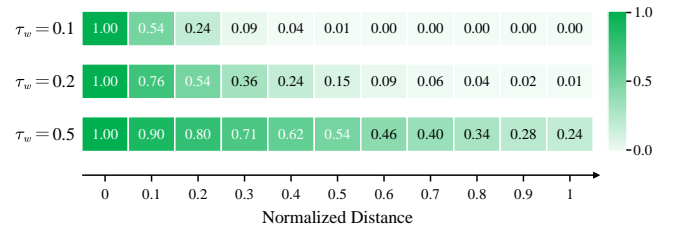


Figure 4: **Soft assignments $w(\cdot, \cdot)$ with different τ_w .** We use heat maps to visualize the soft assignments with different sharpness parameters τ_w . For clarity, we set the upper bound $\alpha = 1$ in the figure. Best viewed in color.

Leveraging the soft assignments for all sample pairs, we propose a soft contrastive loss to refine the traditional hard contrastive loss. Specifically, for a pair of projected embeddings (z_i, \tilde{z}_i) , we first calculate the softmax probability of

the relative similarity among all similarities as:

$$p(z_i, \tilde{z}_i) = \frac{\exp(\text{sim}(z_i, \tilde{z}_i)/\tau_c)}{\sum_{z' \in \mathcal{Z} \setminus \{z_i\}} \exp(\text{sim}(z_i, z')/\tau_c)}, \quad (4)$$

where $\text{sim}(\cdot, \cdot)$ refers to the cosine similarity, and τ_c is a temperature parameter used to adjust the scale. Based on $p(z_i, \tilde{z}_i)$, the soft contrastive loss is then defined as:

$$\mathcal{L}_{C,i} = -\log p(z_i, \tilde{z}_i) - \sum_{\substack{x' \in \Omega \setminus \{x_i, \tilde{x}_i\} \\ z' \in \mathcal{Z} \setminus \{z_i, \tilde{z}_i\}}} w(x_i, x') \cdot \log p(z_i, z'), \quad (5)$$

where $\Omega = \mathcal{X} \cup \tilde{\mathcal{X}}$ represents the union of the data spaces of the original and masked samples. By assigning soft weights to different sample pairs, the model is encouraged to better capture the inherent correlations across different samples. During the training process, the final soft contrastive loss \mathcal{L}_C is computed by summing and averaging $\mathcal{L}_{C,i}$ across all samples within a mini-batch. Notably, when $\forall w(x_i, x') = 0$, the soft contrastive loss reduces to the traditional hard contrastive loss.

Aggregate Reconstruction To further capture the fine-grained relationships between different samples, we incorporate an aggregator for weighted aggregation and reconstruction. Current approaches for masked EEG modeling typically reconstruct the masked portion based on the unmasked portion of a single masked sample (Lan et al. 2024; Pang et al. 2024), following the learning paradigm of MAE (He et al. 2022). However, this single-sample reconstruction strategy overlooks the interactions between samples, leading to a complex and inadequate reconstruction process.

To overcome this limitation, we introduce an aggregator that improves the traditional single-sample reconstruction process. Specifically, we first calculate the cosine similarity between each pair of projected embeddings (z_i, z_j) within a mini-batch, resulting in a similarity matrix \mathcal{S} . Based on the pairwise similarities in \mathcal{S} , the aggregator then performs weighted aggregation of the embedding h_i . The weighted aggregation process is defined as:

$$h_i^r = \sum_{z' \in \mathcal{Z} \setminus \{z_i\}} \left(\frac{\exp(\text{sim}(z_i, z')/\tau_c)}{\sum_{z'' \in \mathcal{Z} \setminus \{z_i\}} \exp(\text{sim}(z_i, z'')/\tau_c)} \cdot h' \right), \quad (6)$$

where $h' \in \mathcal{H} \setminus \{h_i\}$ represents the encoded embedding corresponding to the projected embedding z' , and \mathcal{H} denotes the embedding space of the encoder E . This approach allows for a more comprehensive reconstruction by aggregating complementary information and incorporating similar features from different samples during the reconstruction process, while suppressing interference from irrelevant noise samples. Finally, the reconstructed embedding h_i^r is fed into a lightweight decoder D to obtain the reconstructed sample x_i^r . Following the masked modeling paradigm, we use Mean Square Error (MSE) as the reconstruction loss for model optimization, which is defined as:

$$\mathcal{L}_{R,i} = \|x_i - x_i^r\|_2^2. \quad (7)$$

Similar to the soft contrastive loss \mathcal{L}_C , the final reconstruction loss \mathcal{L}_R is computed by summing and averaging $\mathcal{L}_{R,i}$ across all samples within a mini-batch.

The pre-training process of SCMM During the pre-training process, SCMM is trained by jointly optimizing \mathcal{L}_C and \mathcal{L}_R . The overall pre-training loss is defined as:

$$\mathcal{L} = \lambda_C \mathcal{L}_C + \lambda_R \mathcal{L}_R, \quad (8)$$

where λ_C and λ_R are trade-off hyperparameters, which are adaptively adjusted according to the homoscedastic uncertainty of each loss item. Algorithm 1 details the pre-training process of the proposed SCMM.

Algorithm 1: The pre-training process of SCMM.

Input: Unlabeled pre-training dataset $\mathcal{X} = \{x_i\}_{i=1}^N$. The number of pre-training *epochs*.

The pre-training process:

- 1: Randomly initialize the model parameters θ ;
 - 2: **for** *epoch* = 1 to *epochs* **do**
!All operations are performed within a mini-batch!*
 - 3: Generate the masked sample \tilde{x}_i of each input EEG sample x_i using hybrid masking in **Eq. (1)**;
 - 4: Generate h_i and \tilde{h}_i by feeding x_i and \tilde{x}_i into E ;
 - 5: Generate z_i and \tilde{z}_i by feeding h_i and \tilde{h}_i into P ;
 - 6: Compute the normalized distance $D(x_i, x_j)$ for each pair of samples (x_i, x_j) using **Eq. (2)**;
 - 7: Generate the soft assignment $w(x_i, x_j)$ for each pair of samples (x_i, x_j) using **Eq. (3)**;
 - 8: Compute the soft contrastive loss \mathcal{L}_C using **Eq. (5)**;
 - 9: Compute the pairwise cosine similarity for each pair of projected embeddings (z_i, z_j) ;
 - 10: Generate the reconstructed embedding h_i^r of each h_i through weighted aggregation in **Eq. (6)**;
 - 11: Reconstruct x_i^r by feeding h_i^r into D ;
 - 12: Compute the reconstruction loss \mathcal{L}_R using **Eq. (7)**;
 - 13: Compute the pre-training loss \mathcal{L} using **Eq. (8)**;
 - 14: Update the model parameters θ ;
 - 15: **end for**
 - 16: **return** The pre-trained SCMM model f_θ .
-

Experiments

Datasets

We conduct extensive experiments on three publicly available datasets, SEED (Zheng and Lu 2015), SEED-IV (Zheng et al. 2018), and DEAP (Koelstra et al. 2011), to evaluate the model performance of SCMM. These datasets are diverse in terms of EEG equipment, emotional stimuli, data specifications, labeling approaches and subjects, making them well-suited for assessing the model’s efficacy in cross-corpus EEG-based emotion recognition tasks. In our experiments, we use differential entropy (DE) features as inputs. Detailed descriptions of the datasets and pre-processing procedures are provided in Appendix A.

Methods	Same-Class		Different-Class	
	SEED-IV ³ → SEED ³	SEED ³ → SEED-IV ³	SEED-IV ⁴ → SEED ³	SEED ³ → SEED-IV ⁴
BiDANN (Li et al. 2018)	49.24 / 10.49	60.46 / 11.17	-	-
TANN (Li et al. 2021)	58.41 / 07.16	60.75 / 10.61	-	-
PR-PL (Zhou et al. 2023)*	61.01 / 10.55	58.74 / 10.71	-	-
E ² STN (Zhou et al. 2024)	60.51 / 05.41	61.24 / 15.14	-	-
SimCLR (Tang et al. 2021)*	47.27 / 08.44	46.89 / 13.41	44.19 / 09.28	42.03 / 10.05
Mixup (Wickstrøm et al. 2022)*	56.86 / 16.83	55.70 / 16.28	54.55 / 17.95	45.79 / 15.16
MAE (He et al. 2022)*	<u>86.49 / 10.57</u>	<u>83.87 / 08.53</u>	<u>86.02 / 08.96</u>	<u>76.74 / 09.18</u>
JCFA (Liu et al. 2024a)*	67.53 / 12.36	62.40 / 07.54	65.99 / 14.04	52.67 / 05.86
SCMM (Ours)	91.61 / 07.56 (+05.12)	87.24 / 08.35 (+03.37)	91.26 / 07.91 (+05.24)	80.89 / 08.69 (+04.15)

Table 1: Experimental results on SEED and SEED-IV under two cross-corpus conditions: same-class and different-class. “*” indicates that the results are reproduced by ourselves. A → B denotes that A is the pre-training dataset, while B is the dataset for model fine-tuning and testing. **Best results** are highlighted in bold, while the second-best results are underlined.

Hard \mathcal{L}_C	Soft \mathcal{L}_C	\mathcal{L}_R	Same-Class		Different-Class	
			SEED-IV ³ → SEED ³	SEED ³ → SEED-IV ³	SEED-IV ⁴ → SEED ³	SEED ³ → SEED-IV ⁴
✓			90.08 / 09.24	84.43 / 11.83	90.26 / 08.71	77.79 / 08.04
	✓		90.73 / 08.48	85.07 / 11.05	90.96 / 08.36	78.32 / 07.19
		✓	89.68 / 09.32	84.24 / 11.90	89.45 / 09.10	77.24 / 09.14
✓		✓	90.30 / 07.94	85.95 / 08.74	90.91 / 08.61	79.82 / 07.00
	✓	✓	91.61 / 07.56	87.24 / 08.35	91.26 / 07.91	80.89 / 08.69

Table 2: Ablation study on SEED and SEED-IV under two cross-corpus conditions: same-class and different-class.

Implementation Details

In the pre-training stage, we set r to 0.5 and μ to 0.1 for hybrid masking. We set α to 0.5, τ_w to 0.05, and τ_c to 0.5 for soft CL. The Adam optimizer is utilized with a learning rate of $5e-4$ and a weight decay of $3e-4$. The pre-training process is conducted over 200 epochs with a batch size of 256. We save the parameters θ from the final epoch as the pre-trained model. In the fine-tuning stage, we input the embeddings h_i generated by the encoder E into an emotion classifier consisting of a 2-layer MLP for final emotion recognition. The classifier is optimized using cross-entropy (CE) loss, and the fine-tuning process is conducted over 50 epochs with a batch size of 128. All experiments are conducted using Python 3.9 with PyTorch 1.13 on an NVIDIA GeForce RTX 3090 GPU. Further implementation details and hyperparameter analysis can be found in Appendix B and Appendix E.

Baselines and Experimental Setup

We compare the proposed SCMM against eight competitive baseline methods, including four conventional deep learning methods: BiDANN (Li et al. 2018), TANN (Li et al. 2021), PR-PL (Zhou et al. 2023), and E²STN (Zhou et al. 2024), as well as four self-supervised learning models: SimCLR (Chen et al. 2020; Tang et al. 2021), Mixup (Zhang et al. 2018; Wickstrøm et al. 2022), MAE (He et al. 2022), and JCFA (Liu et al. 2024a). Notably, E²STN and JCFA are specifically designed for cross-corpus EEG-based emo-

tion recognition. To ensure a fair comparison, we adopt a cross-corpus subject-independent protocol in our experiments, consistent with the setup used by JCFA. We evaluate the model performance using the average accuracy and standard deviation (ACC / STD %) across all subjects in the test set. More details about baseline methods and experimental settings are provided in Appendix C.

Experimental Results

Evaluation on the SEED and SEED-IV datasets To fully validate the model performance of SCMM, we conduct extensive experiments under two cross-corpus conditions: (1) same-class and (2) different-class.

(1) For the same-class cross-corpus validation, we conduct two experiments on the SEED and SEED-IV 3-category datasets: pre-training on SEED-IV and fine-tuning on SEED (SEED-IV³ → SEED³), and pre-training on SEED and fine-tuning on SEED-IV (SEED³ → SEED-IV³). In both experiments, all samples corresponding to fear emotions in the SEED-IV dataset are excluded. The left two columns in Table 1 present the comparison results, indicating that SCMM achieves SOTA performance in both experiments. Specifically, our model achieves classification accuracies of 91.61% and 87.24% with standard deviations of 7.56% and 8.35% in the SEED-IV³ → SEED³ and SEED³ → SEED-IV³ experiments, outperforming the second-best method MAE by accuracies of 5.12% and 3.37%, respectively.

Methods	DEAP \rightarrow SEED ³	SEED ³ \rightarrow DEAP (Valence)	SEED ³ \rightarrow DEAP (Arousal)
SimCLR (Tang et al. 2021)*	53.12 / 13.12	53.75 / 03.61	51.79 / 04.54
Mixup (Wickstrøm et al. 2022)*	48.75 / 14.37	60.62 / 08.68	60.11 / 07.69
MAE (He et al. 2022)*	83.69 / 10.10	72.19 / 07.24	70.50 / 06.30
JCFA (Liu et al. 2024a)*	64.69 / 12.28	61.59 / 06.26	61.06 / 07.37
SCMM (Ours)	91.70 / 08.07 (+08.01)	73.96 / 06.75 (+01.77)	72.66 / 05.67 (+02.16)

Table 3: Experimental results for cross-corpus EEG-based emotion recognition on SEED and DEAP.

(2) For the different-class cross-corpus validation, we conduct another two experiments, denoted as SEED-IV⁴ \rightarrow SEED³ and SEED³ \rightarrow SEED-IV⁴. These experiments aim to evaluate the model performance when the pre-training and fine-tuning datasets contain different emotion categories. Experimental results in the right two columns of Table 1 demonstrate that SCMM achieves the best performance in both experiments. Specifically, our model achieves classification accuracies of 91.26% and 80.89% with standard deviations of 7.91% and 8.69% in the SEED-IV⁴ \rightarrow SEED³ and SEED³ \rightarrow SEED-IV⁴ experiments, surpassing the second-best method MAE by 5.24% and 4.15% in accuracies, respectively. Note that the traditional CL-based models SimCLR, Mixup, and JCFA exhibit relatively poor performance, primarily due to their use of raw EEG signals as inputs. In addition, SCMM significantly outperforms the traditional masked modeling framework MAE, highlighting the superiority of SCMM. In summary, extensive experimental results on the SEED and SEED-IV datasets confirm that our model exhibits superior performance in multiple cross-corpus EEG-based emotion recognition tasks.

Ablation study To assess the validity of each module in SCMM, we conduct a comprehensive ablation study on the SEED and SEED-IV datasets. Specifically, we design five different models below. (1) **Hard \mathcal{L}_C** trains the model with only hard contrastive loss. (2) **Soft \mathcal{L}_C** trains the model with only soft contrastive loss. (3) **\mathcal{L}_R** trains the model with only reconstruction loss. (4) **Hard \mathcal{L}_C and \mathcal{L}_R** trains the model using both hard contrastive loss and reconstruction loss. (5) **Soft \mathcal{L}_C and \mathcal{L}_R** trains the model using both soft contrastive loss and reconstruction loss, representing the full model.

Table 2 presents the results of ablation experiments. Specifically, (1) **Hard \mathcal{L}_C** and (2) **Soft \mathcal{L}_C** : the first two models compare the performance of hard CL and soft CL. Experimental results indicate that our well-designed soft contrastive learning effectively improves the classification accuracy. (3) **\mathcal{L}_R** : the third model removes the soft contrastive loss and trains the model with only reconstruction loss. The results show that the model performs worst in the absence of the contrastive learning constraint. (4) **Hard \mathcal{L}_C and \mathcal{L}_R** and (5) **Soft \mathcal{L}_C and \mathcal{L}_R** : the last two models compare the performance when combining hard and soft contrastive loss with reconstruction loss, respectively. Experimental results demonstrate that the full model achieves the best performance in all experiments, indicating that SCMM significantly enhances the model performance and stability by combining soft contrastive learning and aggregate recon-

struction. This improvement is evident under different cross-corpus conditions, demonstrating the feasibility of extending SCMM to real-life aBCI applications.

Discussion

Generalization capability analysis To further validate the generalization capability of SCMM, we conduct additional experiments on the SEED and DEAP datasets under a different-class cross-corpus scenario, denoted as DEAP \rightarrow SEED³, SEED³ \rightarrow DEAP (Valence) and SEED³ \rightarrow DEAP (Arousal). It is notable that the EEG acquisition equipment, emotional stimuli, data specifications, labeling approaches and subjects are completely different between the two datasets. Table 3 presents the experimental results of SCMM compared to existing methods. Specifically, for the DEAP \rightarrow SEED³ experiment, SCMM achieves an accuracy of 91.70% with a standard deviation of 8.07%, outperforming the second-best method MAE by an accuracy of 8.01%. For the SEED³ \rightarrow DEAP (Valence) and SEED³ \rightarrow DEAP (Arousal) experiments, our model achieves classification accuracies of 73.96% and 72.66% with standard deviations of 6.75% and 5.67%, surpassing the second-best method MAE by 1.77% and 2.16% in accuracies. Experimental results demonstrate that the proposed SCMM maintains excellent performance even when the pre-training and fine-tuning datasets are completely different, highlighting its superior generalization capability.

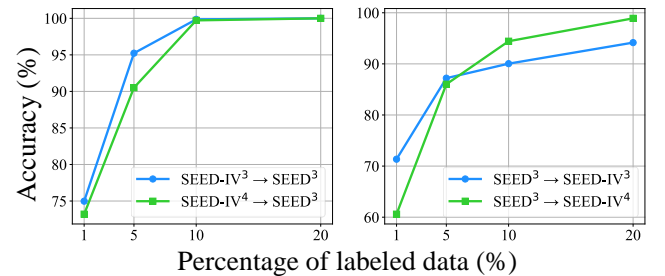


Figure 5: Model performance with limited labeled data for fine-tuning on SEED and SEED-IV.

Model performance with limited fine-tuning data We further explore the model performance of SCMM on the SEED and SEED-IV datasets when fine-tuning labeled data is limited. Specifically, we randomly select 1%, 5%, 10% and 20% of labeled samples from the fine-tuning dataset for

Method	ACC / STD (%)			
	SEED-IV ³ → SEED ³	SEED ³ → SEED-IV ³	SEED-IV ⁴ → SEED ³	SEED ³ → SEED-IV ⁴
OS	91.61 / 07.56	87.24 / 08.35	91.25 / 07.91	80.89 / 08.69
ES	89.99 / 10.25	85.75 / 14.00	90.31 / 08.59	79.04 / 06.95
	DEAP → SEED ³	SEED ³ → DEAP (Valence)	SEED ³ → DEAP (Arousal)	-
OS	91.70 / 08.01	73.96 / 06.75	72.66 / 05.67	-
ES	90.64 / 07.97	72.75 / 07.06	71.58 / 05.72	-

Table 4: Comparison of soft contrastive learning in the original data space (OS) and embedding space (ES).

Strategies	SEED-IV ³ → SEED ³	SEED ³ → SEED-IV ³
Random	90.30 / 08.80	84.63 / 10.99
Channel	90.25 / 08.68	85.91 / 10.97
Hybrid	91.61 / 07.56	87.24 / 08.35

Table 5: Comparative experiments of different masking strategies on the SEED and SEED-IV 3-category datasets.

model fine-tuning, while the remaining samples are used for testing. Figure 5 shows the classification accuracy curves. For the SEED-IV³ → SEED³ and SEED-IV⁴ → SEED³ experiments, SCMM achieves classification accuracies exceeding 70% with only 1% of labeled data. The accuracies significantly improve as the proportion of labeled samples increases, reaching close to 100% with 10% of labeled data. Meanwhile, our model achieves classification accuracies over 60% and 70% with only 1% of labeled data in the SEED³ → SEED-IV³ and SEED³ → SEED-IV⁴ experiments. The classification accuracies exceed 90% when fine-tuning with 10% of labeled samples in both experiments. In summary, experimental results indicate that SCMM maintains superior performance even with limited labeled data for fine-tuning, showing its outstanding robustness and potential in few-shot scenarios. The complete results and computational complexity analysis are provided in Appendix F.

Comparison of different masking strategies To assess the impact of various masking strategies, we conduct comparative experiments on the SEED and SEED-IV 3-category datasets using three strategies: random, channel, and hybrid masking. Table 5 presents the experimental results, showing that the hybrid masking strategy achieves the highest accuracy and the lowest standard deviation in both experiments. This suggests that the integration of different masking approaches significantly improves the model performance and stability. More details on the different masking strategies are presented in Appendix D.

Comparison of soft CL in the original data space and embedding space While soft contrastive learning has been explored across various domains, most methods focus on computing soft assignments for contrastive loss in the embedding space (Dwivedi et al. 2021; Yèche et al. 2021). However, we argue that utilizing similarities in the original

data space offers superior self-supervision and is particularly well-suited for EEG emotional data. To validate this, we conduct additional experiments on the SEED, SEED-IV and DEAP datasets to verify the effectiveness of soft contrastive learning in the original data space. Specifically, we modify the metric function $Dist(\cdot, \cdot)$ to use similarities between projected embeddings, shifting the computation of soft assignments from the original data space to the embedding space. Table 4 presents the experimental results, demonstrating that soft contrastive learning in the original data space consistently outperforms the embedding space in all experiments. Furthermore, this approach allows for pre-computing cosine similarities between original sample pairs offline, thus reducing computational resource requirements and improving training efficiency.

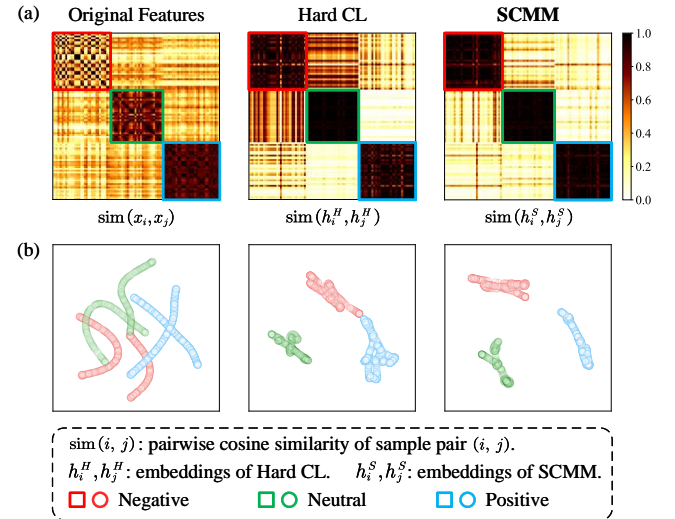


Figure 6: (a) Heat maps of pairwise similarity matrices. (b) t-SNE visualization of the learned embeddings. Best viewed in color. Zoom in for better view.

Visualization To evaluate whether sample-wise relationships are preserved in the encoder, we randomly select 100 test samples from the SEED dataset, and visualize the pairwise cosine similarity between sample pairs. Additionally, we select all test samples of one subject from the SEED

dataset and visualize the learned embeddings of SCMM using t-SNE (Van der Maaten and Hinton 2008). Figure 6(a) presents heat maps of pairwise similarity matrices, where darker colors indicate higher similarity between samples. Traditional hard CL identifies only coarse-grained relationships across samples from different emotion categories, especially for the most challenging-to-recognize negative and neutral emotions. In contrast, SCMM effectively captures the fine-grained relationships between samples of different categories. Moreover, the results of t-SNE visualization in Fig. 6(b) indicate that the proposed SCMM better clusters samples within the same category and increases the inter-class distance compared to traditional hard CL, thus enhancing the classification performance. More visualization results can be found in Appendix G.

Conclusion

This paper proposes a novel self-supervised pre-training framework, **Soft Contrastive Masked Modeling (SCMM)**, for cross-corpus EEG-based emotion recognition. Unlike traditional contrastive learning models, SCMM integrates soft contrastive learning with a hybrid masking strategy to effectively capture the "short-term continuity" characteristics inherent in human emotions, and produce stable and generalizable EEG representations. Additionally, an aggregator is developed to weightedly aggregate complementary information from multiple close samples, thereby enhancing fine-grained feature representation capability in the modeling process. Extensive experiments on three well-recognized datasets show that SCMM consistently achieves SOTA performance in cross-corpus EEG-based emotion recognition tasks under both same-class and different-class conditions. Comprehensive ablation study and parameter analysis confirm the superior performance and robustness of SCMM. Visualization results indicate that our model effectively reduces the distance between similar samples within the same category, and captures more fine-grained relationships across samples. These findings suggest that SCMM enhances the feasibility of extending the proposed method to real-life aBCI applications.

References

- Canal, F. Z.; Müller, T. R.; Matias, J. C.; Scotton, G. G.; de Sa Junior, A. R.; Pozzebon, E.; and Sobieranski, A. C. 2022. A survey on facial emotion recognition techniques: A state-of-the-art literature review. *Information Sciences*, 582: 593–617.
- Chen, T.; Kornblith, S.; Norouzi, M.; and Hinton, G. 2020. A simple framework for contrastive learning of visual representations. In *International Conference on Machine Learning*, 1597–1607. PMLR.
- Chien, W.-S.; Yang, H.-C.; and Lee, C.-C. 2020. Cross corpus physiological-based emotion recognition using a learnable visual semantic graph convolutional network. In *Proceedings of the 28th ACM International Conference on Multimedia*, 2999–3006.
- Davidson, R. J. 1998. Affective style and affective disorders: Perspectives from affective neuroscience. *Cognition & emotion*, 12(3): 307–330.
- Dwibedi, D.; Aytar, Y.; Tompson, J.; Sermanet, P.; and Zisserman, A. 2021. With a little help from my friends: Nearest-neighbor contrastive learning of visual representations. In *Proceedings of the IEEE/CVF International Conference on Computer Vision*, 9588–9597.
- Eldele, E.; Ragab, M.; Chen, Z.; Wu, M.; Kwok, C. K.; Li, X.; and Guan, C. 2021. Time-Series Representation Learning via Temporal and Contextual Contrasting. In *Proceedings of the Thirtieth International Joint Conference on Artificial Intelligence, IJCAI-21*, 2352–2359.
- Gao, P.; Liu, T.; Liu, J.-W.; Lu, B.-L.; and Zheng, W.-L. 2024. Multimodal Multi-View Spectral-Spatial-Temporal Masked Autoencoder for Self-Supervised Emotion Recognition. In *ICASSP 2024-2024 IEEE International Conference on Acoustics, Speech and Signal Processing (ICASSP)*, 1926–1930. IEEE.
- He, K.; Chen, X.; Xie, S.; Li, Y.; Dollár, P.; and Girshick, R. 2022. Masked autoencoders are scalable vision learners. In *Proceedings of the IEEE/CVF Conference on Computer Vision and Pattern Recognition*, 16000–16009.
- He, Z.; Zhong, Y.; and Pan, J. 2022. An adversarial discriminative temporal convolutional network for EEG-based cross-domain emotion recognition. *Computers in Biology and Medicine*, 141: 105048.
- Houben, M.; Van Den Noortgate, W.; and Kuppens, P. 2015. The relation between short-term emotion dynamics and psychological well-being: A meta-analysis. *Psychological bulletin*, 141(4): 901.
- Hu, X.; Chen, J.; Wang, F.; and Zhang, D. 2019. Ten challenges for EEG-based affective computing. *Brain Science Advances*, 5(1): 1–20.
- Koelstra, S.; Muhl, C.; Soleymani, M.; Lee, J.-S.; Yazdani, A.; Ebrahimi, T.; Pun, T.; Nijholt, A.; and Patras, I. 2011. Deap: A database for emotion analysis; using physiological signals. *IEEE Transactions on Affective Computing*, 3(1): 18–31.
- Lan, Y.-T.; Jiang, W.-B.; Zheng, W.-L.; and Lu, B.-L. 2024. CEMOAE: A Dynamic Autoencoder with Masked Channel Modeling for Robust EEG-Based Emotion Recognition. In *ICASSP 2024-2024 IEEE International Conference on Acoustics, Speech and Signal Processing (ICASSP)*, 1871–1875. IEEE.
- Li, R.; Wang, Y.; Zheng, W.-L.; and Lu, B.-L. 2022. A multi-view spectral-spatial-temporal masked autoencoder for decoding emotions with self-supervised learning. In *Proceedings of the 30th ACM International Conference on Multimedia*, 6–14.
- Li, Y.; Fu, B.; Li, F.; Shi, G.; and Zheng, W. 2021. A novel transferability attention neural network model for EEG emotion recognition. *Neurocomputing*, 447: 92–101.
- Li, Y.; Zheng, W.; Cui, Z.; Zhang, T.; and Zong, Y. 2018. A novel neural network model based on cerebral hemispheric asymmetry for EEG emotion recognition. In *IJCAI*, 1561–1567.

- Liu, Q.; Zhou, Z.; Wang, J.; and Liang, Z. 2024a. Joint Contrastive Learning with Feature Alignment for Cross-Corpus EEG-based Emotion Recognition. *arXiv:2404.09559*.
- Liu, Z.; Alavi, A.; Li, M.; and Zhang, X. 2024b. Guidelines for Augmentation Selection in Contrastive Learning for Time Series Classification. *arXiv:2407.09336*.
- Noroozi, F.; Corneanu, C. A.; Kamińska, D.; Sapiński, T.; Escalera, S.; and Anbarjafari, G. 2018. Survey on emotional body gesture recognition. *IEEE Transactions on Affective Computing*, 12(2): 505–523.
- Pang, M.; Wang, H.; Huang, J.; Vong, C.-M.; Zeng, Z.; and Chen, C. 2024. Multi-Scale Masked Autoencoders for Cross-Session Emotion Recognition. *IEEE Transactions on Neural Systems and Rehabilitation Engineering*.
- Radford, A.; Kim, J. W.; Hallacy, C.; Ramesh, A.; Goh, G.; Agarwal, S.; Sastry, G.; Askell, A.; Mishkin, P.; Clark, J.; et al. 2021. Learning transferable visual models from natural language supervision. In *International Conference on Machine Learning*, 8748–8763. PMLR.
- Rayatdoost, S.; and Soleymani, M. 2018. Cross-corpus EEG-based emotion recognition. In *2018 IEEE 28th International Workshop on Machine Learning for Signal Processing (MLSP)*, 1–6. IEEE.
- Russell, J. A. 1980. A circumplex model of affect. *Journal of personality and social psychology*, 39(6): 1161.
- Ryumina, E.; Dresvyanskiy, D.; and Karpov, A. 2022. In search of a robust facial expressions recognition model: A large-scale visual cross-corpus study. *Neurocomputing*, 514: 435–450.
- Schuller, B.; Vlasenko, B.; Eyben, F.; Wöllmer, M.; Stuhlsatz, A.; Wendemuth, A.; and Rigoll, G. 2010. Cross-corpus acoustic emotion recognition: Variances and strategies. *IEEE Transactions on Affective Computing*, 1(2): 119–131.
- Shen, X.; Liu, X.; Hu, X.; Zhang, D.; and Song, S. 2022. Contrastive learning of subject-invariant EEG representations for cross-subject emotion recognition. *IEEE Transactions on Affective Computing*, 14(3): 2496–2511.
- Singh, Y. B.; and Goel, S. 2022. A systematic literature review of speech emotion recognition approaches. *Neurocomputing*, 492: 245–263.
- Tang, C. I.; Perez-Pozuelo, I.; Spathis, D.; and Mascolo, C. 2021. Exploring Contrastive Learning in Human Activity Recognition for Healthcare. *arXiv:2011.11542*.
- Van der Maaten, L.; and Hinton, G. 2008. Visualizing data using t-SNE. *Journal of Machine Learning Research*, 9(11).
- Wang, Y.; Zhang, B.; and Tang, Y. 2024. DMMR: Cross-subject domain generalization for EEG-based emotion recognition via denoising mixed mutual reconstruction. In *Proceedings of the AAAI Conference on Artificial Intelligence*, volume 38, 628–636.
- Wickstrøm, K.; Kampffmeyer, M.; Mikalsen, K. Ø.; and Jenssen, R. 2022. Mixing up contrastive learning: Self-supervised representation learning for time series. *Pattern Recognition Letters*, 155: 54–61.
- Yèche, H.; Dresdner, G.; Locatello, F.; Hüser, M.; and Rätsch, G. 2021. Neighborhood contrastive learning applied to online patient monitoring. In *International Conference on Machine Learning*, 11964–11974. PMLR.
- Yue, Z.; Wang, Y.; Duan, J.; Yang, T.; Huang, C.; Tong, Y.; and Xu, B. 2022. Ts2vec: Towards universal representation of time series. In *Proceedings of the AAAI Conference on Artificial Intelligence*, volume 36, 8980–8987.
- Zhang, H.; Cisse, M.; Dauphin, Y. N.; and Lopez-Paz, D. 2018. mixup: Beyond Empirical Risk Minimization. *arXiv:1710.09412*.
- Zhang, K.; Wen, Q.; Zhang, C.; Cai, R.; Jin, M.; Liu, Y.; Zhang, J. Y.; Liang, Y.; Pang, G.; Song, D.; et al. 2024. Self-supervised learning for time series analysis: Taxonomy, progress, and prospects. *IEEE Transactions on Pattern Analysis and Machine Intelligence*.
- Zhang, X.; Zhao, Z.; Tsiligkaridis, T.; and Zitnik, M. 2022. Self-supervised contrastive pre-training for time series via time-frequency consistency. *Advances in Neural Information Processing Systems*, 35: 3988–4003.
- Zhang, Z.; Liu, Y.; and Zhong, S.-h. 2022. GANSER: A self-supervised data augmentation framework for EEG-based emotion recognition. *IEEE Transactions on Affective Computing*, 14(3): 2048–2063.
- Zhang, Z.; Weninger, F.; Wöllmer, M.; and Schuller, B. 2011. Unsupervised learning in cross-corpus acoustic emotion recognition. In *2011 IEEE Workshop on Automatic Speech Recognition & Understanding*, 523–528. IEEE.
- Zhao, L.-M.; Yan, X.; and Lu, B.-L. 2021. Plug-and-play domain adaptation for cross-subject EEG-based emotion recognition. In *Proceedings of the AAAI Conference on Artificial Intelligence*, volume 35, 863–870.
- Zheng, W.-L.; Liu, W.; Lu, Y.; Lu, B.-L.; and Cichocki, A. 2018. Emotionmeter: A multimodal framework for recognizing human emotions. *IEEE Transactions on Cybernetics*, 49(3): 1110–1122.
- Zheng, W.-L.; and Lu, B.-L. 2015. Investigating critical frequency bands and channels for EEG-based emotion recognition with deep neural networks. *IEEE Transactions on Autonomous Mental Development*, 7(3): 162–175.
- Zhong, P.; Wang, D.; and Miao, C. 2020. EEG-based emotion recognition using regularized graph neural networks. *IEEE Transactions on Affective Computing*, 13(3): 1290–1301.
- Zhou, R.; Zhang, Z.; Fu, H.; Zhang, L.; Li, L.; Huang, G.; Li, F.; Yang, X.; Dong, Y.; Zhang, Y.-T.; et al. 2023. PR-PL: A novel prototypical representation based pairwise learning framework for emotion recognition using EEG signals. *IEEE Transactions on Affective Computing*, 15(2): 657–670.
- Zhou, Y.; Li, F.; Li, Y.; Ji, Y.; Zhang, L.; and Chen, Y. 2024. Enhancing Cross-Dataset EEG Emotion Recognition: A Novel Approach with Emotional EEG Style Transfer Network. *arXiv:2403.16540*.

Appendix A Datasets

A.1 Dataset Description

We conduct extensive experiments on three well-recognized datasets, SEED (Zheng and Lu 2015), SEED-IV (Zheng et al. 2018), and DEAP (Koelstra et al. 2011), to evaluate the model performance of SCMM in cross-corpus EEG-based emotion recognition tasks. Table 6 provides a detailed description of the three datasets.

(1) **SEED** (Zheng and Lu 2015) was developed by Shanghai Jiao Tong University. The dataset used a 62-channel ESI NeuroScan System based on the international 10-20 system to record EEG signals from 15 subjects (7 males and 8 females) under different video stimuli at a sampling rate of 1kHz. Each subject participated in 3 sessions. In each session, each subject was required to watch 15 movie clips consisting of 3 different emotional states: negative, neutral and positive. Each emotional state contains a total of 5 movie clips, corresponding to 5 trials.

(2) **SEED-IV** (Zheng et al. 2018) used the same EEG acquisition equipment as the SEED dataset, but with different video stimuli, emotion categories and subjects. The dataset recorded EEG signals from 15 subjects under different video stimuli at a sampling rate of 1kHz. Each subject participated in 3 sessions. In each session, each subject was required to watch 24 movie clips containing 4 different emotions: sad, neutral, fear and happy. Each emotion contains a total of 6 movie clips, corresponding to 6 trials.

(3) **DEAP** (Koelstra et al. 2011) was constructed by Queen Mary University of London. The dataset used a 128-channel Biosemi ActiveTwo System to record EEG signals from specific 32 channels of 32 subjects (16 males and 16 females) while watching 40 one-minute music videos at a sampling rate of 512Hz. The 40 one-minute videos elicited different emotions according to the valence-arousal dimension. Specifically, the valence-arousal emotional model, first proposed by Russell (Russell 1980), places each emotional state on a two-dimensional scale. The first dimension represents valence, ranging from negative to positive, and the second dimension represents arousal, ranging from calm to exciting. Participants rated valence and arousal using a continuous scale of 1 to 9 after watching each video clip.

A.2 Pre-processing Procedures

For the SEED and SEED-IV datasets, the raw EEG signals were initially downsampled to 200Hz and filtered through a bandpass filter of 0.3-50Hz to filter noise and remove artifacts. Then, the data were divided into multiple non-overlapping segments using sliding windows of 1 second for SEED and 4 seconds for SEED-IV, respectively. After that, we extracted differential entropy (DE) features for each channel of each segment at five frequency bands: Delta (1-4Hz), Theta (4-8Hz), Alpha (8-14Hz), Beta (14-31Hz), and Gamma (31-50Hz). Finally, the DE features from 62 channels and 5 bands were formed into a feature matrix of shape 62×5 , which serves as input to the SCMM model. The extraction of DE features can be expressed as:

$$DE(x) = \frac{1}{2} \log(2\pi e \sigma^2), \quad (9)$$

Here, x represents an EEG signal segment of a specific length that approximately obeys a Gaussian distribution $N(\mu, \sigma^2)$, where σ denotes the standard deviation of x , and e is the Euler constant.

For the DEAP dataset, the raw EEG signals were first downsampled to 128Hz and denoised by a bandpass filter of 4-45Hz. Subsequently, the data were segmented into multiple non-overlapping segments using a sliding window of 1s. Similar to the SEED and SEED-IV datasets, DE features were extracted for each channel of each segment at five frequency bands. Finally, the DE features from 32 channels and 5 bands were formed into a feature matrix of shape 32×5 as input to the model. During the experiments, we divided the continuous labels using a fixed threshold of 5 to convert them to binary classification tasks (low / high).

A.3 Handling Different Number of Channels

Since the SEED-series datasets and the DEAP dataset contain different numbers of electrodes (channels), we require channel processing before inputting DE features into the model. Specifically, we consider the fine-tuning dataset as an anchor. When the number of channels in the fine-tuning dataset is less than in the pre-training dataset, we select data from the corresponding channels in the pre-training dataset and drop the data from the redundant channels as inputs (e.g., pre-training on SEED and fine-tuning on DEAP). Conversely, when the number of channels in the fine-tuning dataset is greater than in the pre-training dataset, we fill the missing channel data with zeros in the pre-training dataset to match the fine-tuning dataset (e.g., pre-training on DEAP and fine-tuning on SEED).

Appendix B Implementation Details

To reduce computational load while maintaining model performance, we adopt a lightweight design for each module of SCMM. Specifically, we use a 3-layer 1D CNN for the encoder E and a 2-layer MLP for the projector P . For the lightweight decoder D , we utilize a single-layer MLP for reconstruction. Regarding hyperparameter selection in the pre-training stage, we set r to 0.5 and μ to 0.1 for hybrid masking, i.e., the percentage of random masking and channel masking is 0.9 and 0.1, respectively. We use the negative of cosine similarity as the metric function $Dist(\cdot, \cdot)$, and we set α to 0.5, τ_w to 0.05 and τ_c to 0.5 for soft contrastive learning. We use Adam as the optimizer with a learning rate of 5×10^{-4} and an L2-norm penalty coefficient 3×10^{-4} . The pre-training process is conducted over 200 epochs with a batch size of 256. We save the model parameters θ from the final epoch as the pre-trained SCMM. In the fine-tuning stage, we input the encoded embeddings h_i into a classifier consisting of a 2-layer fully connected network for final emotion recognition. The Adam optimizer is utilized with a learning rate of 5×10^{-4} and a weight decay of 3×10^{-4} . The number of fine-tuning epochs is set to 50 for the SEED and SEED-IV datasets and 500 for the DEAP dataset, with a batch size of 128. For efficient deployment and testing of the model, the pre-trained SCMM is optimized solely using cross-entropy loss during fine-tuning. All experiments

Datasets	Subjects	Sessions \times Trials	Channels	Sampling Rate	Classes
SEED	15	3×15	62	1kHz	3 (Negative, Neutral, Positive)
SEED-IV	15	3×15	62	1kHz	4 (Sad, Neutral, Fear, Happy)
DEAP	32	1×40	32	512Hz	Valence: 1 - 9, Arousal: 1 - 9

Table 6: Detailed description of the experimental datasets.

	Pre-training	Fine-tuning
Encoder	3-layer 1D CNN	
Projector	2-layer MLP	
Decoder	single-layer MLP	
Classifier	-	2-layer MLP
Masking ratio r	0.5	-
Threshold μ	0.1	-
Upper bound α	0.5	-
Sharpness τ_w	0.05	-
Temperature τ_c	0.5	-
Epoch	200	50, 500
Optimizer	Adam	
Learning rate	5×10^{-4}	
Weight decay	3×10^{-4}	
Batch size	256	128

Table 7: Hyperparameter settings of SCMM.

are conducted using Python 3.9 with PyTorch 1.13 on an NVIDIA GeForce 3090 GPU.

Appendix C Baseline Methods and Experimental Settings

C.1 Baseline Methods

We compare the proposed SCMM against eight competitive methods, including four traditional deep learning methods: BiDANN (Li et al. 2018), TANN (Li et al. 2021), PR-PL (Zhou et al. 2023) and E²STN (Zhou et al. 2024), as well as four self-supervised learning models: SimCLR (Chen et al. 2020; Tang et al. 2021), Mixup (Zhang et al. 2018; Wickstrøm et al. 2022), MAE (He et al. 2022) and JCFA (Liu et al. 2024a). Details of the eight baseline methods are summarized as follows.

- **BiDANN** (Li et al. 2018): The bi-hemispheres domain adversarial neural network mapped the EEG data of both left and right hemispheres into discriminative feature spaces separately to address domain shifts in EEG-based emotion recognition tasks.

- **TANN** (Li et al. 2021): The transferable attention neutral network is a novel transfer learning methods which learned the discriminative information from EEG signals using local and global attention mechanisms.
- **PR-PL** (Zhou et al. 2023): The prototypical representation based pairwise learning framework adopted pairwise learning to model the relative relationships between EEG sample pairs in terms of prototypical representations, addressing the critical issues of individual differences and noise labels in cross-subject scenarios.
- **E²STN** (Zhou et al. 2024): The emotional EEG style transfer network integrated content information from the source domain with style information from the target domain, achieving superior performance in cross-corpus EEG-based emotion recognition tasks.
- **SimCLR** (Chen et al. 2020; Tang et al. 2021): A seminal work in self-supervised contrastive learning, first proposed for computer vision, has been extended to human activity recognition.
- **Mixup** (Zhang et al. 2018; Wickstrøm et al. 2022): A novel CL-based data augmentation method that aimed to correctly predict the mixing proportion of two samples, has been applied to time series analysis.
- **MAE** (He et al. 2022): A groundbreaking work in the field of mask modeling, which proposed to reconstruct the masked portion based on the unmasked portion of the masked sample, has achieved remarkable success in a wide range of fields.
- **JCFA** (Liu et al. 2024a): The joint contrastive learning framework performed joint contrastive learning across two domains to synchronize the time- and frequency-based embeddings of the same EEG sample in the latent time-frequency space, achieving state-of-the-art performance in cross-corpus scenarios.

To ensure a fair comparison, we adopt the same encoder, projector, decoder, and classifier structures for SimCLR, Mixup and MAE as used in SCMM. We use the default hyperparameters reported in the original paper for all methods in our experiments, unless otherwise specified. Additionally, for BiDANN, TANN, PR-PL, E²STN, MAE, and SCMM, the input samples are preprocessed 1-s DE features. In contrast, SimCLR, Mixup, and JCFA use preprocessed 1-s EEG signals as inputs, in accordance with the specific design of each model.

C.2 Experimental Settings

We adopt a cross-corpus subject-independent experimental protocol in the experiments, following the setup used in

JCFA. Specifically, samples from one dataset are used for pre-training, while samples of each subject from another dataset are used individually for fine-tuning and testing. During the fine-tuning process, we employ a leave-trials-out setting, where samples from a part of trials in each session of each subject in the fine-tuning dataset are used for fine-tuning, and the remaining trials are used for testing. For example, SCMM is pre-trained on the SEED-IV dataset and fine-tuned on the SEED dataset. The allocation of samples for fine-tuning/testing is as follows: 9/6 for the SEED dataset, 12/6 for the SEED-IV 3-category dataset, 16/8 for the SEED-IV 4-category dataset, and 24/16 for the DEAP dataset. This approach effectively avoids information leakage. The detailed experimental settings and data division for pre-training and fine-tuning are summarized in Table 8.

Appendix D Masking Strategy

This paper introduces a novel hybrid masking strategy to generate diverse masked samples by considering both channel and feature relationships. To compare our approach with traditional masking strategies, we explore three different masking rules: random masking, channel masking, and hybrid masking. Figure 3 illustrates the difference between these three masking strategies.

(1) **Random Masking:** Generate masks using a binomial distribution to randomly mask samples in the feature dimension, setting the values of the masked features to zero.

(2) **Channel Masking:** Generate masks using a binomial distribution to randomly mask samples in the channel dimension, setting the values of all features within the masked channels to zero.

(3) **Hybrid Masking:** Generate a probability matrix using a uniform distribution that proportionally mixes masks generated from random masking and channel masking.

Our proposed hybrid masking strategy is highly flexible and can be extended to various datasets by integrating multiple masking strategies in different ratios, which is exceptionally suitable for data with rich semantic information. This approach effectively generates more diverse masked samples, encouraging the model to comprehensively capture the inherent relationships of the data.

Appendix E Hyperparameter Analysis

We conduct comprehensive experiments to verify the hyperparameter sensitivity of SCMM on the SEED and SEED-IV 3-category datasets. The hyperparameters examined include the masking ratio r , probability threshold μ , metric function $Dist(\cdot, \cdot)$, upper bound α , sharpness τ_w , and temperature τ_c . The complete experimental results are presented in the following sections.

E.1 Masking Ratio

Table 9 shows the model performance in the $SEED-IV^3 \rightarrow SEED^3$ and $SEED^3 \rightarrow SEED-IV^3$ experiments when using different masking ratios (0.1, 0.25, 0.5, and 0.75). Experimental results demonstrate that the proposed SCMM consistently achieves the best performance when the masking ratio is set to $r = 0.5$.

E.2 Probability Threshold

Table 10 presents the model performance using different probability thresholds (ranging from 0 to 1) for hybrid masking. Here, $\mu = 0$ refers to the exclusive use of the random masking strategy, while $\mu = 1$ indicates the exclusive use of the channel masking strategy. Experimental results show that SCMM achieves the best performance in the $SEED-IV^3 \rightarrow SEED^3$ and $SEED^3 \rightarrow SEED-IV^3$ experiments when the probability threshold is set to $\mu = 0.1$ (i.e., the ratio of random masking and channel masking is 9:1).

E.3 Metric Function

We evaluate the model performance of SCMM using different metric functions in soft assignments $w(\cdot, \cdot)$. Experimental results in Table 11 indicate that SCMM performs best on the SEED and SEED-IV 3-category datasets when cosine similarity is used as the metric function.

E.4 Upper Bound

We assess the impact of different upper bounds on calculating soft assignments $w(\cdot, \cdot)$. To restrict the soft assignments to the range of 0 to 1, we explore the model performance of SCMM with upper bounds of 0.25, 0.5, 0.75, and 1. Experimental results in Table 12 illustrate that the proposed SCMM achieves the best performance in the $SEED-IV^3 \rightarrow SEED^3$ experiment when the upper bound is set to $\alpha = 0.5$.

E.5 Sharpness

Table 13 explore the impact of different sharpness parameters in the $SEED-IV^3 \rightarrow SEED^3$ experiment, as shown in Table 13. Experimental results indicate that our model achieves the best performance with a sharpness parameter of $\tau_w = 0.05$.

E.6 Temperature

We conduct comparison experiments on the SEED and SEED-IV 3-category datasets to explore the impact of temperature parameter on model performance. Experimental results in Table 14 show that SCMM consistently achieves the best performance in both experiments when the temperature parameter is set to $\tau_c = 0.5$.

F Model Performance and Computational Complexity Analysis of SCMM

To investigate the trade-off between model performance and computational complexity in few-shot scenarios, we assess the classification accuracy, time cost, and the number of trainable parameters of SCMM when fine-tuning with limited labeled data. Experimental results in Table 15 show that the model performance of SCMM significantly improves as the number of fine-tuning labeled samples increases. Meanwhile, the inference time cost remains low due to our lightweight design. Additionally, our model achieves superior classification performance in cross-corpus EEG-based emotion recognition tasks with very few parameters. In summary, the proposed SCMM effectively balances model performance and computational complexity.

Evaluations	Scenarios	Pre-training	Fine-tuning / Testing
Same-Class	SEED-IV ³ → SEED ³	SEED-IV, 3-category	SEED: 9 / 6 trials in each session per subject
	SEED ³ → SEED-IV ³	SEED	SEED-IV, 3-category: 12 / 6 trials in each session per subject
Different-Class	SEED-IV ⁴ → SEED ³	SEED-IV, 4-category	SEED: 9 / 6 trials in each session per subject
	SEED ³ → SEED-IV ⁴	SEED	SEED-IV, 4-category: 16 / 8 trials in each session per subject
	DEAP → SEED ³	DEAP	SEED: 9 / 6 trials in each session per subject
	SEED ³ → DEAP (Valence)	SEED	DEAP (Valence): 24 / 16 trials per subject
	SEED ³ → DEAP (Arousal)	SEED	DEAP (Arousal): 24 / 16 trials per subject

Table 8: Pre-training and fine-tuning scenarios under two conditions for cross-corpus EEG-based emotion recognition.

Ratio	ACC / STD (%)	
	SEED-IV ³ → SEED ³	SEED ³ → SEED-IV ³
0.1	91.19 / 08.07	85.05 / 11.68
0.25	91.50 / 07.69	85.28 / 09.91
0.5	91.61 / 07.56	87.24 / 08.35
0.75	90.24 / 08.08	83.49 / 13.19

Table 9: Hyperparameter sensitivity analysis of masking ratio r on SEED and SEED-IV.

G Visualization

G.1 Intra- and Inter-Class Similarities

To assess the quality of the embeddings learned by SCMM, we randomly select one subject from the SEED dataset, and calculate both the average intra- and inter-class cosine similarities between the learned embeddings of all test samples, as shown in Fig. 7. It is evident that the proposed SCMM produces embeddings with higher intra-class similarity compared to traditional hard contrastive learning. In addition, the average inter-class similarity of the embeddings learned by SCMM is significantly lower than that of hard CL. In summary, visualization results confirm that the soft contrastive learning strategy designed in SCMM effectively clusters samples within the same category while distinctly separating samples from different categories, thus enhancing the model’s discriminative capabilities.

G.2 Reconstruction Quality

To verify the effectiveness of the aggregator designed in SCMM, we compare the reconstruction quality of the single-sample reconstruction paradigm (MAE) with the aggregate reconstruction paradigm (SCMM) on the DEAP dataset. For clarity, we flatten both the original input sample and the reconstructed sample into one-dimensional vectors with dimensions $C \times F$ (channels \times features). The results depicted in Fig. 8 illustrate that our model achieves lower reconstruction loss (MSE) and better sample reconstruction.

Threshold	ACC / STD (%)	
	SEED-IV ³ → SEED ³	SEED ³ → SEED-IV ³
0 (Random)	90.30 / 08.80	84.63 / 10.99
0.1	91.61 / 07.56	87.24 / 08.35
0.2	90.93 / 08.18	86.51 / 08.44
0.3	90.84 / 07.70	86.66 / 09.98
0.4	89.34 / 08.70	86.94 / 09.81
0.5	91.00 / 08.22	87.16 / 11.09
0.6	89.93 / 08.90	85.83 / 09.65
0.7	91.08 / 07.64	85.14 / 11.60
0.8	89.52 / 08.29	86.10 / 12.48
0.9	89.42 / 08.18	86.05 / 11.75
1 (Channel)	90.25 / 08.68	85.91 / 10.97

Table 10: Hyperparameter sensitivity analysis of threshold μ on SEED and SEED-IV.

Metrics	ACC / STD (%)	
	SEED-IV ³ → SEED ³	SEED ³ → SEED-IV ³
Manhattan	90.09 / 09.06	85.83 / 11.14
Euclidean	90.86 / 08.57	85.40 / 13.51
Cosine	91.61 / 07.56	87.24 / 08.35

Table 11: Hyperparameter sensitivity analysis of metric function $Dist(\cdot, \cdot)$ on SEED and SEED-IV.

Upper Bound	ACC / STD (%)
	SEED-IV ³ → SEED ³
0.25	91.21 / 08.54
0.5	91.61 / 07.56
0.75	91.12 / 08.25
1	90.50 / 08.00

Table 12: Hyperparameter sensitivity analysis of upper bound α in the SEED-IV³ → SEED³ experiment.

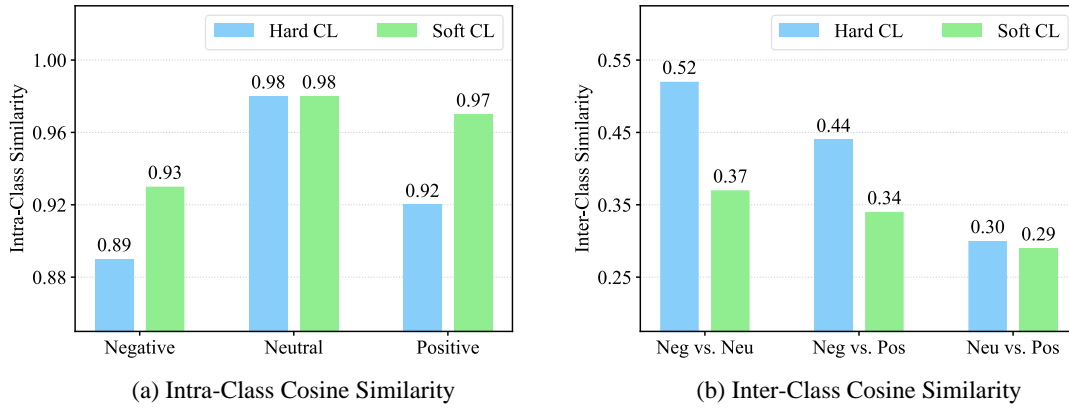


Figure 7: **Intra- and inter-class cosine similarities of embeddings learned by hard CL and soft CL.** (a) is the average intra-class cosine similarity, and (b) is the average inter-class cosine similarity. Best viewed in color.

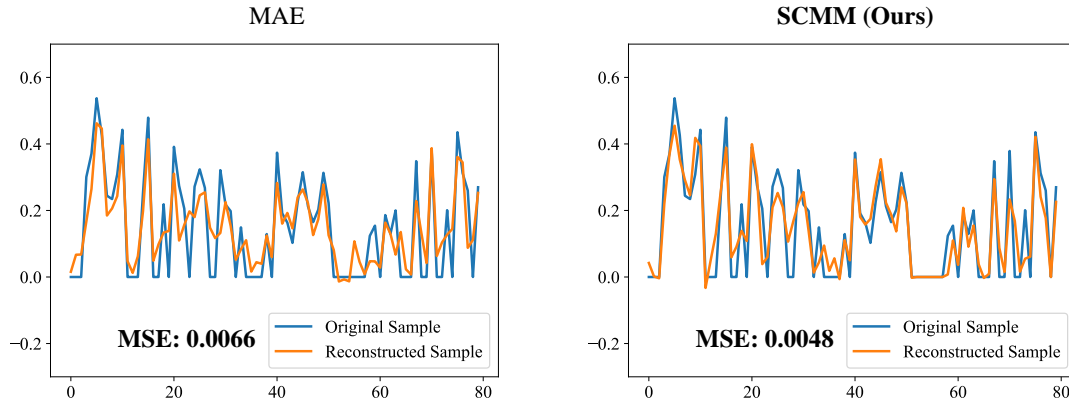


Figure 8: **Comparison of reconstruction quality.** We visualize the reconstruction results to compare the single-sample reconstruction paradigm (MAE) with the aggregate reconstruction paradigm (SCMM). This case is from the DEAP dataset. Best viewed in color.

Sharpness	ACC / STD (%)
	SEED-IV ³ → SEED ³
0.01	90.93 / 09.13
0.05	91.61 / 07.56
0.1	91.08 / 09.00
0.2	90.59 / 07.40
0.5	90.63 / 09.16
1	90.09 / 08.62
2	89.58 / 09.26

Table 13: Hyperparameter sensitivity analysis of sharpness τ_w in the SEED-IV³ → SEED³ experiment.

Temperature	ACC / STD (%)	
	SEED-IV ³ → SEED ³	SEED ³ → SEED-IV ³
0.05	90.97 / 08.17	85.95 / 11.14
0.2	91.16 / 07.85	86.82 / 11.46
0.5	91.61 / 07.56	87.24 / 08.35
2	90.62 / 08.66	86.73 / 10.18

Table 14: Hyperparameter sensitivity analysis of temperature τ_c on SEED and SEED-IV.

Metrics	1% of labeled data			
	SEED-IV ³ → SEED ³	SEED ³ → SEED-IV ³	SEED-IV ⁴ → SEED ³	SEED ³ → SEED-IV ⁴
ACC / STD (%)	74.98 / 17.00	71.35 / 16.29	73.20 / 16.09	60.59 / 23.72
Time Cost (s)	232.35	97.11	232.35	130.47
	5% of labeled data			
	SEED-IV ³ → SEED ³	SEED ³ → SEED-IV ³	SEED-IV ⁴ → SEED ³	SEED ³ → SEED-IV ⁴
ACC / STD (%)	95.23 / 06.98	87.20 / 16.12	90.51 / 12.43	86.01 / 09.76
Time Cost (s)	240.48	100.23	240.48	132.90
	10% of labeled data			
	SEED-IV ³ → SEED ³	SEED ³ → SEED-IV ³	SEED-IV ⁴ → SEED ³	SEED ³ → SEED-IV ⁴
ACC / STD (%)	99.86 / 00.31	90.04 / 16.94	99.72 / 00.80	94.43 / 05.60
Time Cost (s)	250.81	102.03	250.81	135.67
	20% of labeled data			
	SEED-IV ³ → SEED ³	SEED ³ → SEED-IV ³	SEED-IV ⁴ → SEED ³	SEED ³ → SEED-IV ⁴
ACC / STD (%)	100.0 / 00.00	94.16 / 08.52	100.0 / 00.00	98.91 / 02.62
Time Cost (s)	267.21	105.48	267.21	139.31
Model Parameters: 1.52 M				

Table 15: Model performance and computational complexity of SCMM when fine-tuning with limited labeled data (1%, 5%, 10%, and 20%) on SEED and SEED-IV.